Talanta 116 (2013) 488–494

Contents lists available at ScienceDirect

Talanta

journal homepage: www.elsevier.com/locate/talanta

Centrifugal microfluidic platform for radiochemistry: Potentialities for the chemical analysis of nuclear spent fuels

Anthony Bruchet [a], Vélan Taniga [b], Stéphanie Descroix [b], Laurent Malaquin [b], Florence Goutelard [c], Clarisse Mariet [a,*]

[a] CEA/DPC/SEARS/LANIE, French Alternative Energies and Atomic Energy Commission, Saclay, France
[b] MMBM Group, Institut Curie Research Center, CNRS UMR 168, Paris, France
[c] CEA/DPC/SEARS/LASE, French Alternative Energies and Atomic Energy Commission, Saclay, France

ARTICLE INFO

Article history:
Received 22 February 2013
Received in revised form
25 June 2013
Accepted 30 June 2013
Available online 13 July 2013

Keywords:
Microfluidics
Centrifugal microfluidic platform
Centrifuge flow
Radiochemistry
Monolithic stationary phase
Anion-exchange separation
Nuclear spent fuel.

ABSTRACT

The use of a centrifugal microfluidic platform is for the first time reported as an alternative to classical chromatographic procedures for radiochemistry. The original design of the microfluidic platform has been thought to fasten and simplify the prototyping process with the use of a circular platform integrating four rectangular microchips made of thermoplastic. The microchips, dedicated to anion-exchange chromatographic separations, integrate a localized monolithic stationary phase as well as injection and collection reservoirs. The results presented here were obtained with a simplified simulated nuclear spent fuel sample composed of non-radioactive isotopes of Europium and Uranium, in proportion usually found for uranium oxide nuclear spent fuel. While keeping the analytical results consistent with the conventional procedure (extraction yield for Europium of ≈97%), the use of the centrifugal microfluidic platform allowed to reduce the volume of liquid needed by a factor of ≈250. Thanks to their unique "easy-to-use" features, centrifugal microfluidic platforms are potential successful candidates for the downscaling of chromatographic separation of radioactive samples (automation, multiplexing, easy integration in glove-boxes environment and low cost of maintenance).

© 2013 Elsevier B.V. All rights reserved.

1. Introduction

Materials control and accountancy (MC&A) is a vital task within the nuclear industry, demanded by both international treaty and safety guidelines for nuclear power plants. The precise and accurate chemical analysis of nuclear spent fuel (NSP) (determination of the concentration levels of Uranium, Plutonium and some Fission Products, (FP)) represents a critical part of MC&A and plays an essential role in designing future nuclear fuels cycle, reprocessing as well as for waste management. Such chemical analysis remains challenging because of the numerous steps involved: namely dissolution of a fuel rod, chemical treatment of the obtained acidic solution and chromatographic isolation of targeted elements before high precision mass spectrometry measurements. To obtain uncertainty at several per mil level on isotope ratio using Thermo-Ionization Mass Spectrometry (TIMS) or Multi-Collection Inductively Coupled Plasma Mass Spectrometry (MC-ICP-MS) [1–3], mono-elemental samples are mandatory. Obtaining pure fractions of each radionuclides (through chromatographic separations) remains difficult because NSP samples exhibit an extreme chemical diversity stemming from several schemes of neutron capture, fissions or activation reactions that occur in reactors. This leads to the formation of the so-called transuranium radionuclides (Np, Pu, Am, Cm) as well as a wide variety of fission products (FP) constituted of lanthanides (Nd, Sm, Eu, Gd), alkalines (Cs) and alkaline earth metals (Sr). Their concentration ranges usually from a few pg L^{-1} for some fission products up to g L^{-1} level for Uranium while Plutonium concentration depends on the type of fuel (uranium oxide UO*x*) and ranges from 0.1 to 10 mg L^{-1}. Moreover, after a prolonged stay in a nuclear reactor, NSP samples are very 'hot' products and their analyses require appropriate shielding level to reduce the dose uptake for the analyst such as remote handling in hot cells or extreme dilution.

In this context, the integration of several analytical steps (sample preparation followed by chromatographic separation for example) along with the miniaturization allowed by microfluidics appears to be a valuable alternative to standard procedures. Downscaling of radioactive sample volume (or quantity) could lead to an almost proportional reduction of radiations [4], and thus, to a considerable decrease of the shielding level needed. For example, considering a nitric acid solution in which nuclear spent fuel is dissolved, a 1000-fold volume reduction makes the analysis possible in glove-boxes instead of hot cells. Moreover, the use of

* Corresponding author. Tel.: +33 1 69 08 49 60; fax: +33 1 69 08 94 75.
E-mail address: clarisse.mariet@cea.fr (C. Mariet).

0039-9140/$ - see front matter © 2013 Elsevier B.V. All rights reserved.
http://dx.doi.org/10.1016/j.talanta.2013.06.064

Micro-Total Analysis Systems (or Micro-TAS) integrating sample chemical treatment and chromatographic separations before mass spectrometry analysis could reduce both the overall time of analysis as currently most of these steps remain hand-performed and the volume of wastes produced that is especially critical for radiochemistry.

Among the numerous formats of microsystems, centrifugal microfluidic platforms (also called Lab-on-CD or lab-on-a-disc [5,6]) are attractive candidates to carry out the chromatographic separation step involved in the chemical analysis of NSP samples because fluid handling is "simply" provided by the use of the centrifuge force while no connection to external pumps or power supplies is needed. This simplifies tremendously the use of the whole system [5] as well as its maintenance which are mandatory features of any miniaturized devices to be implemented in highly radioactive area such as glove boxes. Moreover, parallel sample processing and/or multiplexed analysis can be also considered, as many individual structures can typically be replicated radially within a single disc [6]. This represents a clear advantage on standard procedures both in terms of reproducibility and time of analysis as several samples are processed in the very same manner (using the same disc). Additional forces resulting from spinning can be also used advantageously: for instance, the flow direction, controlled by the Coriolis force, can be exploited to collect different fractions in separated reservoirs [7]. Alternately spinning the disc in opposite directions (i.e. clockwise and anti-clockwise) is also a simple and efficient fluid mixing method [8].

These unique features have contributed to the expansion of centrifugal microfluidic platforms interest in the past 15–20 years within both academic and industrial communities [5,9–11]. Among them, solid phase extraction and/or chromatographic separation deserve special considerations because both require the integration, in the device, of a stationary phase which selectively retains targeted analytes. Columns packed with micro-particles have been often used as they are natural counterparts of usual chromatographic columns [12,13]. In that case, slurry of silica particles are introduced in the microchips through centrifugal force and the bed is retained using frits, quartz wool or restriction at the end of the column [12–16]. Curiously, the integration of monolithic stationary phase in centrifugal microfluidic platforms remains rather unexplored despite an increasing number of publications demonstrating their interest in microsystems within diverse microfluidic platforms [16–19]. To our knowledge, only one study has recently reported the integration of a monolith in a centrifugal microfluidic platform [11,20]. In this case, a methacrylate monolith was synthesized by microwave-initiated polymerization and subsequently used for protein purification process including binding, elution, isolation, and detection. Nevertheless, the assessment of centrifugal flow rate through the monolithic column is not reported.

Toward the conception of a fully integrated Lab-on-CD for radiochemical analysis, this study focused on the design of a centrifugal device dedicated to the core of NSP samples analysis process: the anion-exchange chromatographic separation. This step leads to the obtaining of three purified fraction respectively containing Uranium, Plutonium and all the FP. Nevertheless, as the setup was not implemented in a controlled area yet, a proof of concept has been demonstrated using a non-radioactive NSP simulated sample composed of traces of Europium (representative of FP elements) in an Uranium matrix (≈97% of a spent fuel matrix). The efficient separation, thanks to the precise and reproducible control of the centrifuge flow rate, leads to the isolation of a pure fraction of Europium with analytical performances similar to the one obtained with standard separation procedures.

2. Experimental

2.1. Chemicals and reagents

Ethylene dimethacrylate (EDMA), glycidylmethacrylate (GMA), triethylamine (TEA), 1,4-butanediol and azobisisobutyronitrile (AIBN) were obtained from Acros Organics (Noisy-Le-Grand, France). All HPLC-grade solvents (1-propanol, acetonitrile, and ethanol), 3-(trimethoxysilyl)-propyl methacrylate and triethylamine (TEA) were from Sigma-Aldrich (Isle-d'Abeau, France). Pellets (type 6013) and films (F09-61-1, 381 μm thick) of Cyclo-Olefin Copolymer (COC) were obtained from Topas (Polyplastics Co., Germany).

All aqueous solutions were prepared with 18-MΩ deionized water produced by a Milli-Q water purification system (Millipore, Bedford, MA). HNO_3 68% and HCl Ultrex 37% were purchased from Sigma-Aldrich (Isle-d'Abeau, France).

2.2. Fabrication of the centrifugal microfluidic platform

Unlike the majority of the centrifugal microfluidic platforms previously described where the fluidic features are fully integrated in the disc itself, we chose to manufacture rectangular shape microchips mounted on a circular rotating platform. This specific configuration provides a quick and flexible approach to design and fabricate microchips especially in combination with the thermoforming method described thereafter. Microchips were fabricated in COC thermoplastic material that was chosen because of its high chemical resistance (to organic and aqueous solutions even the highly acid solutions and irradiation), high mechanical stability (the material withstands high temperature and pressure) and its good optical transmittance at 365 nm [20] used for the synthesis of the monolithic column (see Section 2.2.4).

2.2.1. Instrumentation

The circular platform has been machined in polyether ether ketone (PEEK) by Somecap (France) in order to satisfy the constraints of chemical resistance (originating from the HCl mobile phases), weight (acceleration torque) and dimensions of the microchips (7 cm × 2.2 cm). The platform can hold four microchips at a time (Fig. 1a). The centrifuge motion of the platform was driven by a servo motor (Yaskawa SGMAV 01ADA61) with corresponding motor controller (Servopack SGDV R90A01A). The latter was used to control the spindle speed, acceleration, deceleration rates and absolute position of the disc. The software Sigmawin+ was used to program individual spin profiles.

2.2.2. Design of the microchips

The microfluidic channels and reservoirs were designed to allow both an easy integration of the separation column (synthesis and functionalization of the monolith (step 1)) and a reproducible and accurate flow handling through centrifugation (step 2). Fig. 1b shows a detailed view of the microchip design where E, C and R stand respectively for access ports, channels and reservoirs. The dimensions of the reservoir R1 (13 mm × 0.35 = 45 μL) and the channel C1 (500 μm × 200 μm × 2.5 cm = 2.5 μL) were adapted for the target ion-exchange separation. Channels C2 and C3 are used respectively as restriction channel (100 μm × 200 μm × 0.5 cm, expected to strengthen the mechanical stability of the column) and vent channel (used only during centrifuge experiments). Reservoirs R2 and R3 dimensions were designed to accommodate to standard chromatographic connections (Upchurch Scientific).

2.2.3. Thermoforming of the microchips

A large variety of methods can be found within the literature regarding the fabrication of microfluidic platforms considering

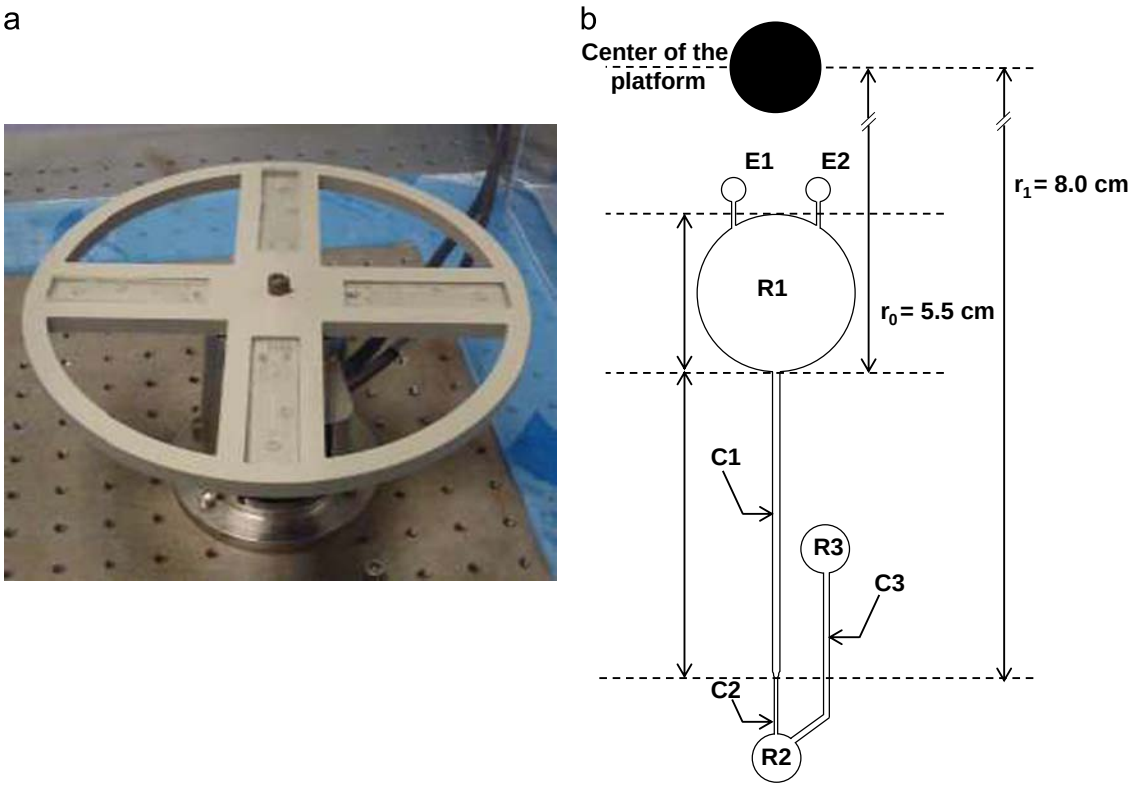

Fig. 1. (a) Centrifugal microfluidic platform including: the rotor securely affixed onto an aluminum chuck, the machined PEEK holding platform and four inserted microchips. (b) Design of the microchips: C1 ion-exchange column, C2 restriction channel, C3 vent channel, R1 injection reservoir, R2 collection reservoir and chromatographic connection, R3 vent and chromatographic connection, E1 entry port and E2 vent port of the injection reservoir.

both standard chips and lab on a CD. Most of the techniques used for channel formation in Lab-on-CD devices [21,22,23] (computer numerical control (CNC) micromilling [8,26], xurography [10,24], lamination [25], laser ablation, soft lithography, hot embossing, injection molding and, thermoforming) leave open channels, which have to be closed by an additional layer [9]. The device enclosing may be performed either by thermal, adhesive, mechanical-based bonding techniques or a combination thereof. In this study, we chose a combination of simple and low cost methods adapted to rapid prototyping of thermoplastic materials: hot embossing and thermal bonding and pressure assisted thermal bonding.

The master mold used for the replication of the chip was obtained by micromilling (MiniMill/3 (Minitech)) starting from a 5 mm thick aluminum plate. The designs of the device as well as the preparation of the milling process were prepared using Catia software. The device consists in two parts (Fig. 1b): (a) the top chip layer is a 381 μm thick film of COC 6013 and was used to ensure the device sealing, and (b) the bottom chip layer that contains the microfluidic channels, the injection and vent holes was prepared as follows (Fig. 2): 20 g of COC 6013 pellets (glass transition temperature T_g 130 °C), previously washed with isopropanol (1 h of sonication), were placed in the molding chamber consisting of a metal holder, the master mold and flat aluminum block that was used as a counter mold. The amount of COC was adjusted for the fabrication of a 7×7 cm^2 and 5 mm thick micro-system. Molding was performed on a thermalized hydraulic press (Atlas Series, Specac). The parts were first heated at 170 °C. The molding step was further carried out using an equivalent load of 1 T (over 10 cm circular plates) for 5 min. The samples were cooled down to room temperature while keeping the pressure constant and finally demolded. Injection inlets, collection reservoir and vent of microchip were created by manual milling using a 4.2 mm HSS (Presto) drill and a tap M5-IS02 (Presto) allowing the integration of commercial chromatographic connections (IDEX Health & Science). The two layers (a) and (b) were washed with isopropanol under ultrasound. In order to perform chip bonding, a thin layer of hexadecane/cyclohexane (25:75 v/v) mixture was deposited on the surface of (b) using a cotton swab. After a quick drying using pressurized air, the thin layer (a) was deposited on (b) and the set was placed in the thermalized hydraulic press at a pressure of 2 T for 10–15 min at 110 °C to ensure contact uniformity and an efficient sealing of the channels.

2.2.4. Integration of the ion-exchange column

The integration of the ion-exchange column was achieved with the photo-induced free radical polymerization of a monolithic copolymer of GMA and EDMA (functionalized thanks to the reactivity of its epoxy groups toward ternary amine molecules [27,28]). The photo-induced polymerization allowed the precise localization of the monolith in the channel C1 while simultaneously ensuring its anchorage to the COC micro-channel walls, as previously described [26].

The porogenic mixture was made up of 52.4% (v/v) 1-propanol, 38.2% (v/v) 1,4-butanediol and 9.4% (v/v) water. The monomer mixture, constituted of 75.4% w/w GMA and 24.6% w/w EDMA, was then dissolved in the porogenic one at a ratio of 49.9:50.1 v/v. AIBN (2.5% w/w of monomers) was used as radical photoinitiator. The polymerization mixtures were introduced in the micro-channel, through the port E1 by pressure using a micropipette. The microchip was inserted into a photo-mask (allowing only the channel C1 to be illuminated) and subsequently irradiated at 365 nm during 30 min (Bio-link cross-linker, VWR International, Strasbourg, France). The irradiation power (P=2.8 mW cm^{-2}) has been adjusted to the use of the photo-mask to compensate the loss

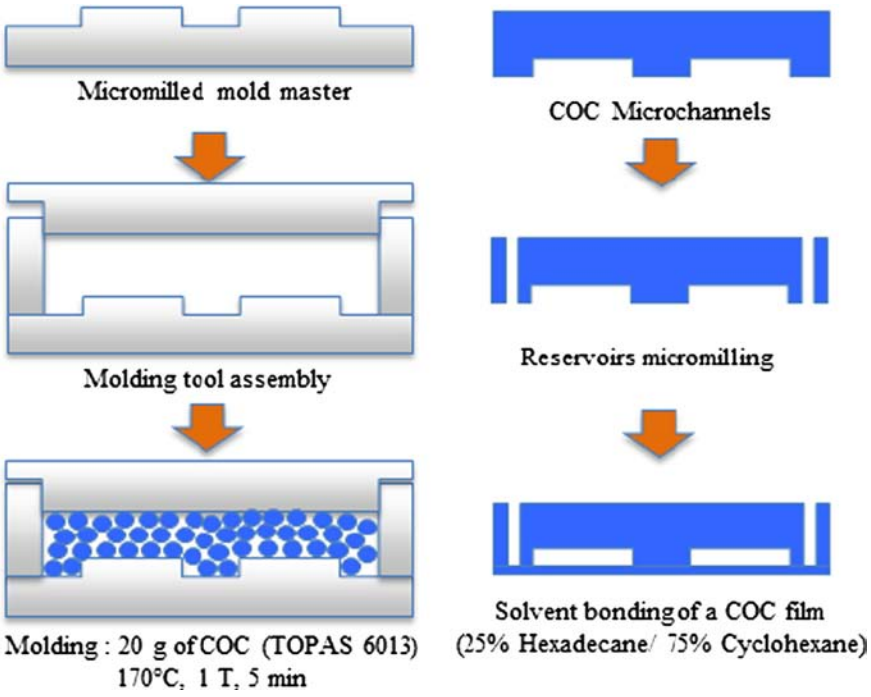

Fig. 2. COC microdevices fabrication process. Microchannels are produced through hot embossing of COC pellets on a micromilled aluminum mold (T=170 °C, 1 T, 5 min). The device is finally sealed with a COC film using a solvent assisted bonding process.

of incident UV light inherent to its use. After the synthesis, the monolith was rinsed with acetonitrile at 1 μL min^{-1} for 6 h before subsequent functionalization as detailed in Section 2.2.5. The validation of its structural properties was assessed by the measurement of its hydrodynamic permeability K_0 (≈5.1 × 10^{-14} m^2) as well as with Scanning Electron Microscopy images [26,28,29].

2.2.5. Functionalization of the monolith

Functionalization of the monolith was performed as previously described for capillary columns [28]. Briefly, monolithic columns were slowly filled under hydrodynamic flow (≈1 μL min^{-1}) with a solution of TEA diluted in 50/50 (v/v) ethanol/water solvent mixture (TEA/solvent 1/10 (v/v)). The functionalization was carried out under dynamic conditions with a flow rate of 1 μL min^{-1} at a temperature of 85 °C for 4 h. The resulting 3-triethylammonium-2-hydroxy-propyl functionalized monolith was then rinsed at 1 μL min^{-1} successively with ethanol, ethanol/water 50:50 v/v and water for 6 h. The resulting ion-exchange capacity of the column was measured, as previously described [28], to be 300 μmol g^{-1} (equivalent to 86 nmol μL^{-1}).

2.3. Separation procedure using the centrifugal microfluidic platform

2.3.1. Sample and mobile phases preparation

The samples were daily prepared by diluting standard SPEX solutions of Europium and Uranium into concentrated HCl solutions to obtain a final HCl concentration of 9.5 mol L^{-1} (1 mL samples of 0.25 mg L^{-1} and 630 mg L^{-1} of Europium and Uranium respectively). No more precautions were taken to control the oxidation state of Europium and Uranium, expected to be (III) and (VI) respectively in concentrated HCl [30,31]. Mobile phases were daily prepared by adding 37% Ultrex HCl to ultra-pure water.

2.3.2. Centrifuge flow rate measurement

Centrifuge flow through the ion-exchange column was determined, after given spinning times, by measuring the level of liquid in the injection reservoir with a scale of 0.5 mm divisions which allowed measuring the meniscus position to the nearest 0.25 mm. To enhance the accuracy of the measurements, and due to the circular shape of the reservoir, the level of mobile phase was monitored only after a prolonged spinning time (between 10 min and 60 min, depending on the mobile phase and the rotational frequency), minimizing the experimental error.

2.3.3. Separation procedure

The separation procedure is detailed in Table 1. Prior to the anion-exchange separation, the monolithic column was first washed with 45 μL of HCl 1 mol L^{-1} to ensure a complete saturation of ion-exchange sites with chloride anions. Then the column was slowly conditioned with 45 μL of HCl 9.5 mol L^{-1} to obtain a homogeneous and reproducible polymeric structure all along the column (a pronounced swelling occurs at high ionic strength, see Section 3.1). The minimal injection volume (V_{inj}=5 μL) was defined to collect at the end of the experiment 1 ng of purified Eu (required for ICP-MS measurements) from an initial sample concentration of 0.25 mg L^{-1} (estimating an extraction of at least 80%).

The pipetting operations were conducted by inserting the micropipette tip into the port E1 while leaving the port E2 open and carefully injecting the liquid into the reservoir. At the end of the experiment, the column was stored hydrated in an aqueous solution of 0.1 mol L^{-1} HCl.

2.4. Detection of Europium and Uranium with ICP-MS

Inductively coupled plasma mass spectrometry (ICP-MS) measurements have been performed using a quadrupole ICP-MS spectrometer 7700× (Agilent Technologies) equipped with a concentric nebulizer. Instrumental parameters were fixed as indicated in Table 2. For the ICP-MS method, calibration solutions were prepared from certified stock multi-elemental 1000 mg g^{-1} solutions SPEX, (JobinYvon). Analytical calibration standards were prepared daily over the range of 0–20 ng g^{-1} for Eu and U by suitable serial dilutions of multi-element stock solution in 2% (v/v)

Table 1
Procedure for the ion-exchange separation of Europium and Uranium using the centrifugal microfluidic platform.

	Step number	Pipetting operation	Centrifuge driven operation
Washing	1	Inject 45 μL of HCl 1 mol L^{-1} into R1	
	2		Centrifuge at 1500 rpm for ~13 min
Conditioning	3	Inject 45 μL of HCl 9.5 mol L^{-1} into R1	
	4		Centrifuge at 1500 rpm for ~30 min
Loading	5	Inject 5 μL of HCl 9.5 mol L^{-1} into R1	
	6		Centrifuge at 900 rpm for 10 min
Separation	7	Inject 10 μL of HCl 9.5 mol L^{-1} into R1	
	8		Centrifuge at 900 rpm for 16 min (volume of Europium fraction collected = 8 μL)
	9		Centrifuge at 900 rpm for 4 min (emptying the injection reservoir)
	10	Inject 45 μL of HCl 1 mol L^{-1} into R1	
	11		Centrifuge at 900 rpm for 9 min (volume of Uranium fraction collected = 11 μL)
	12		Centrifuge at 1500 rpm for 10 min (emptying the injection reservoir and washing the column)

Table 2
Typical ICP-MS operating conditions.

ICP parameters	
Plasma	Argon
rf power	1500 W
Cooling gas flow rate	15 L min^{-1}
Auxiliary gas flow rate	0.9 L min^{-1}
Nebulizer gas flow rate	1.05 L min^{-1}
Mass spectrometer	
Interface vacuum	1.9 hPa
Analyzer vacuum	3.8 10^{-7} hPa
Acquisition parameters	
Full quantitative scan mode	
Dwell time	10 ms/element
Replicates	5
Ion collecting mode	Pulse counting

HNO_3. ^{158}Gd and ^{209}Bi were used as internal standards at the concentration of 2 ng g^{-1}. The internal standards were diluted from 1000 mg g^{-1} stock standard. Sensitivity maximization and short-term stability tests were performed on a daily basis using a 1 ng g^{-1} solution of U and In.

3. Results and discussion

3.1. Assessment of centrifuge flow rate in the microchips

An accurate flow rate assessment is essential to obtain efficient and reproducible chromatographic separations. Excessive band broadening and/or partial loss of sample (due to the use of either too low and too high flow rates respectively) can be avoided by choosing appropriate flow rates. This guarantees the obtaining of high extraction yields, high purity of fractions and optimal separation time [32]. A previous evaluation of the chromatographic performances of the anion-exchange monolith in capillary columns [29] showed that the highest separation efficiency was achieved for a flow rate of 0.1 μL min^{-1}. To apply the same pressure, and considering the dimensions of the micro-column, a flow rate around 1.3 μL min^{-1} has to be obtained.

Hence, evaluation of the flow rate ranges achievable with the centrifugal microfluidic platform has been carried out with water (used as a reference for the characterization of the swelling of the monolithic column, see later in this section) and HCl 9.5 M used as mobile phase used for the loading and elution steps (Fig. 3). When applying rotational frequency ranging from 250 to 1500 rpm, flow rates of water were between 0.1 and 3.3 μL min^{-1} while using HCl 9.5 M the flow rates generated are slightly lower with a maximum (at 1500 rpm) of 1.4 μL min^{-1}. The latter is in agreement with the flow rate expected to give the best separation performances as mentioned above.

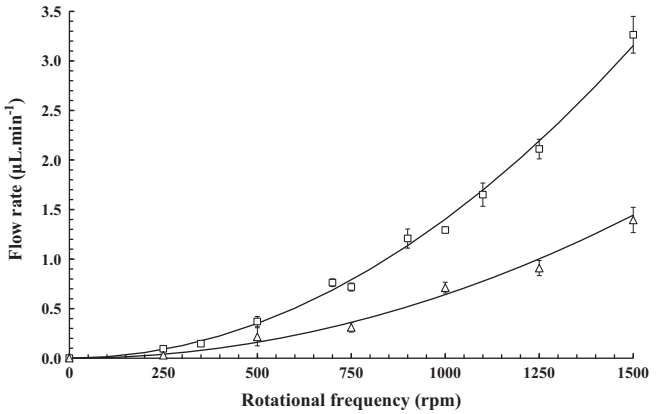

Fig. 3. Experimental flow rates measured with water (□) and HCl 9.5 M (Δ) through the monolithic column as a function of the rotational frequency ω. Fitted curves are obtained using Eq. (1) with appropriate values for each different mobile phase. Error bars have been calculated from data obtained from three microsystems.

Fitting of experimental flow rate curves has been achieved using the expression of centrifuge flow rate described by Penrose et al. [14] adjusted to the case of monolithic columns:

$$F = \frac{\rho h w \bar{r} \Delta r}{2\eta} \omega^2 \frac{(r_{H,\text{monolith}})^2 \varepsilon}{L_{\text{eff}}} \quad (1)$$

where η is the dynamic viscosity and ρ is the density of the mobile phase, h and w respectively are the height and the width of the column and ω is the angular velocity. The terms $\bar{r}$ and Δr are respectively the average distance of the liquid in the microchannel from the center of rotation and the radial extent of liquid. They are obtained using the following equations:

$$\bar{r} = \frac{r_1 + (r_0 - H)}{2} \quad (2)$$

$$\Delta r = r_1 - (r_0 - H) \quad (3)$$

where r_0 and r_1 are respectively the inner and the outer radii of the flowing liquid, and H, the head of the liquid being pumped through the column as described Fig. 1b. The terms $r_{\text{H,monolith}}$, ε and L_{eff} are specific to the anion-exchange monolith and corresponds respectively to its hydraulic radius, external porosity and effective length ($L_{\text{eff}} = LT$ where L is the column length and T is the tortuosity factor accounting for the tortuosity of the liquid flow paths through the monolith [10]). Because these parameters can hardly be predicted in the case of polymeric monoliths [29,33], the last term of Eq. (1) has been empirically adjusted to fit

experimental curves of centrifuge flow. Values obtained for water and HCl 9.5 M mobile phases were respectively 4.6×10^{-13} m^2 and 3.2×10^{-13} m^2. The lower value for HCl 9.5 M illustrates the swelling of the polymeric stationary phase due to the presence of the ionized poorly crosslinked oligomers at the surface of the polymeric monolith [34]. Well-known for conventional polymeric ion-exchange particles, this phenomenon (for the first time characterized on a polymeric monolith using centrifugation) illustrates the necessity of conditioning the monolithic column with HCl 9.5 M to obtain reproducible solid–liquid exchange surfaces and thus reproducible separations. To get such reproducible conditions, a prolonged conditioning step has been applied before any anion-exchange separation as detailed in Section 2.

3.2. Anion-exchange chromatographic separation of simulated NSP samples

As previously mentioned, the chemical analysis of NSP samples starts with the anion-exchange separation of the two main constituents (Uranium and Plutonium) from the fission products (mainly lanthanides, Am and Cm). However, for safety management concerns, the centrifugal microfluidic platform is not installed in a controlled area yet, allowing its use only with non-radioactive isotopes. Hence, the evaluation of the micro-device potentialities has been carried out with the separation of Europium (whose chromatographic behavior is expected to be the same as the other trivalent lanthanides, Cm (III) and Am (III) [31]).

First we have been investigating the anion-exchange properties of the monolith by measuring the distribution coefficients K_D, for both Europium and Uranium (Table 3) and compared the results obtained with a conventional stationary phase. As detailed in the introduction, during the sample loading step in HCl 9.5 M chloride complexes of U (VI) (mostly $UO_2Cl_3^-$, [30]) should be retained on the column while cationic and/or neutral chloride complexes of Europium (III) ($EuCl_x^{3-x}$, x=0–3, [31]) should be eluted. Thereafter, during the elution step U (VI) should be eluted in HCl 1 M under neutral and/or cationic forms. Hence K_D have been measured in HCl 9.5 M for Eu (III) and U (VI) as well as in HCl 1 M for U (VI) and compared to values obtained for commonly used anion-exchange particles (particles AG1 × 8 from Bio-Rad) as shown in Table 3. As expected, K_D values around 0 mL g^{-1} were found for Eu (III) in HCl 9.5 M and U (VI) in HCl 1 M for both materials. However, the K_D of U (VI) on the monolith was 16.5 times lower than on the AG1 × 8 particles. Since both materials are ammonium strong anion-exchanger, this ratio can only be explained by the large difference between the anion-exchange total capacities of the two materials: 2700 μmol g^{-1} and 300 μmol g^{-1} for the AG1 × 8 particles and the monolith respectively (measured as previously described [28]).

Table 3
Distribution coefficients of U (VI) and Eu (III) in HCl 1 mol L^{-1} (mobile phase used for the elution of Uranium) and HCl 9.5 mol L^{-1} (mobile phase used during the loading step and the elution of Europium) on AG1 × 8 particles (used in our standard procedure) and on the synthetized monolith.

	K_D U (VI) (mL g^{-1})[a]		K_D Eu (III) (mL g^{-1})[a]
	HCl 1 mol L^{-1}	HCl 9.5 mol L^{-1}	HCl 9.5 mol L^{-1}
Particles AG1 × 8 (Bio-rad)	≈0	1125 ± 10	≈0
Monolith[b]	≈0	68 ± 5	≈0

[a] K_D values were determined with batch experiments after 12 h of contact with a solution to solid ratio of 5 g L^{-1}. After shaking for 12 h, the solid was centrifuged and an aliquot of the supernatant was measured by ICP-MS as described in Section 2.

[b] Anion-exchange monoliths used for K_D measurements were synthesized and functionalized as previously described [28]

Despite the relatively low K_D of U(VI) on the monolith, the separation protocol applied with the centrifugal microfluidic platform was kept identical to the standard procedure developed and routinely used at the laboratory with conventional packed columns (Table 4) allowing the comparison of the two methods. The simulated NSP samples contained Eu (III) at traces level in a U (VI) matrix, prepared in HCl 9.5 M. The concentrations of both elements have been selected to simulate the composition of an uranium oxide NSP sample 630 mg L^{-1} and 0.250 mg L^{-1} respectively for Uranium and Europium concentrations corresponding to an initial ratio [U]/[Eu] of 2520.

The separation with the centrifugal microfluidic platform was performed with an angular velocity of 900 rpm, corresponding to a flow rate of 0.5 μL min^{-1}. Table 4 compares the analysis time, volume of liquid handled and analytical performances obtained with the standard method and the microfluidic device. The extraction yield, calculated as the ratio of the quantities of Europium loaded on the column and measured in the collected fraction, was 94 ± 5% (assuming an error of 5% on the loading volume), in accordance with the expected value. Moreover, the ICP-MS trace-analysis allowed certifying the concentration of Uranium to be below 0.1% of the initial loaded quantity. Finally, a decontamination factor for Europium, DF (Eu), has been estimated using the following expression:

$$DF(Eu) = \frac{[U]_{sample}/[Eu]_{sample}}{[U]_{collected}/[Eu]_{collected}} \quad (4)$$

where $[U]_{sample}$ and $[Eu]_{sample}$ are respectively the initial concentrations of Uranium and Europium while $[U]_{collected}$ and $[Eu]_{collected}$ are respectively the concentrations of Uranium and Europium measured in the collected fraction. The estimated DF for Europium was equal to 45,000 (calculated assuming a concentration of Uranium equal to the LOD of the ICP-MS method). This value compares favorably with the DFs obtained with our standard procedure or found in the literature [35,36].

Even, if the total analysis time remained longer than for the standard procedure (Table 4), further experiments are ongoing with the use of higher rotational frequencies (higher flow rates) and with the use of four microchips at a time. Moreover, the total volume of liquid handled 69 μL compared to the 18 mL with conventional method highlighted the potentialities of the

Table 4
Chromatographic procedure used for the separation of Europium and Uranium using the standard columns packed with AG1 × 8 particles and the centrifugal microfluidic platform integrating the monolithic column.

Operation	Column packed with AG1 × 8 particles		Centrifugal microfluidic platform	
	Volume used (mL)	Operation time (min)[a]	Volume used (mL)	Operation time (min)[b]
Conditioning	10	20	0.045	30
Loading	1	2	0.005	10
Collection of the Europium fraction	4	8	0.008	16
Collection of the Uranium fraction	3	6	0.011	9
Total volume (mL)	18	36	0.069	65
Europium decontamination factor, DF(Eu)	≈100,000		≥45,000[c]	

[a] Assuming a flow rate of ≈0.5 mL min^{-1}.

[b] For a rotational frequency of 900 rpm, except for the conditioning step, done at 1500 rpm.

[c] Calculated assuming a concentration of Uranium in the Europium fraction equal to the LOD of ^{238}Uranium obtained with the ICP-MS

centrifugal microfluidic platform for the drastic reduction of highly radioactive liquid wastes.

4. Conclusion

Centrifugal microfluidic platforms offer great level of freedom of design along with an accurate control of flow thanks to the centrifugal force. Centrifuge flow management was also chosen since it allowed hydrochloric acid mobile phases up to 9.5 M to percolate through the stationary phase avoiding the use of any external pumping devices. The developed prototype, voluntarily simplified, has been designed to demonstrate its ability to be used as centrifugal microfluidic platforms for radiochemistry applications. In this study, it has been applied to chromatographic separation of NSP samples. The use of a monolithic anion-exchange stationary phase allowed generating appropriate flow rates while using relatively low rotational frequencies. Its swelling when exposed to HCl 9.5 M has been characterized using centrifuge flow illustrating the necessity of a controlled conditioning step to obtain reproducible separations. Finally, this work demonstrates the potentialities of centrifugal microfluidic platforms as a viable alternative to standard procedure for chromatographic anion-exchange separations with high extraction yield (94% for Europium) along with high decontamination factors. Their use for radiochemistry applications could lead to critical improvements of the analytical workflow for the nuclear industry namely (1) fewer manipulations and increased throughput when implemented in glove-box; (2) the reduction in solid wastes generated per analytical cycle; (3) the reduction in liquid wastes generated per analytical cycle; (4) an ease of automation and multiplexing; and (5) limited installation and maintenance costs.

Acknowledgment

The authors are extremely grateful to Rémy Fert and Benoit Lemaire, micro-engine workshop, of the Institut Curie Research Center, for their work in micro-fabrication of the mold. Their implication was greatly appreciated. Jérome Randon and Vincent Dugas, TECHSEP Laboratory of the Institute for analytical Sciences (I.S.A), Lyon (France), are acknowledged for discussions and experimental contributions to the synthesis of the monolith.

References

[1] A.N. Halliday, D.C. Lee, J.N. Christensen, M. Rehkamper, W. Yi, X.Z. Luo, C.M. Hall, C.J. Ballentine, T. Pettke, C. Stirling, Geochim. Cosmochim. Acta 62 (1998) 919–940.
[2] F. Vanhaecke, L. Balcaen, D. Malinovsky, J. Anal. At. Spectrom. 24 (2009) 863.
[3] L. Yang, Mass Spectrom. Rev. 28 (2009) 990.
[4] G. Janssens-Maenhout, Nanotechnol. Perceptions 3 (2007) 183–192.
[5] M. Madou, J. Zoval, G. Jia, H. Kido, J. Kim, N. Kim, Annu. Rev. Biomed. Eng. 8 (2006) 601–628.
[6] M. Amasia, M. Madou, Bioanalysis 2 (10) (2010) 1701–1710.
[7] D. Mark, S. Haeberle, T. Metz, S. Lutz, J. Ducrée, R. Zengerle, F. Von Stettenin, Tucson, AZ, 611–614.
[8] A. Kazarine, M. Kong, E.J. Templeton, E.D. Salin, Anal. Chem. 84 (16) (2012) 6939–6943.
[9] J. Zoval, M. Madou, IEEE Proceedings. 92(1) 2004, 140–153.
[10] R. Gorkin, J. Park, J. Siegrist, M. Amasia, B. Seok Lee, J.-M. Park, J. Kim, H. Kim, M. Madou, Y.-K. Cho, Lab Chip 10 (2010) 1758–1773.
[11] M. Vazquez, D. Brabazon, F. Shang, J.O. Omamogho, J.D. Glennon, B. Paull, Trends Anal. Chem. 30 (10) (2011) 1575–1586.
[12] J.P. Lafleur, Hybrid Microscale Analytical Methods for Environmental Analysis, McGill University Montreal, Quebec, Canada, 2009.
[13] A. Penrose, P. Myers, K. Bartle, S. McCrossen, Analyst 129 (2004) 704–709.
[14] Y. Lu, Y. Xia, Luo, Microfluid. Nanofluid. 10 (2011) 1079–1086.
[15] M. Gong, P.W. Bohn, J.V. Sweedler, Anal. Chem. 81 (2009) 2022–2026.
[16] V. Augustin, G. Proczek, S. Descroix, J. Dugay, M.-C. Hennion, J. Sep. Sci. 30 (2007) 2858–2865.
[17] P.A. Levkin, S. Eeltink, T.R. Stratton, R. Brennen, K.M. Robotti, H. Yin, K. Killeen, F. Svec, J.M.J. Fréchet, J. Chromatogr. A 1200 (2008) 55–61.
[18] G. Proczek, V. Augustin, S. Descroix, M.-C. Hennion, Electrophoresis 30 (2009) 515–524.
[19] K.M. Robotti, H. Yin, R. Brennen, L. Trojer, K. Killeen, J. Sep. Sci. 32 (2009) 3379–3387.
[20] K. Faure, M. Albert, V. Dugas, G. Crétier, R. Ferrigno, P. Morin, J.-L. Rocca, Electrophoresis 29 (24) (2008) 4948–4955.
[21] E.A. Moschou, A.D. Nicholson, G. Jia, J. Zoval, M. Madou, L.G. Bachas, S. Daunert, Anal. Bioanal. Chem. 385 (2006) 596–605.
[22] P. Nunes, P. Ohlsson, O. Ordeig, J.P. Kutter, Microfluid. Nanofluid. 9 (2010) 145–161.
[23] J.P. Lafleur, E.D. Salin, J. Anal. At. Spectrom. 24 (2009) 1511–1516.
[24] D. Bartholomeusz, D.R. Boutté, J. Andrade, J. Microelectromech. Syst. 14 (6) (2005) 1364–1374.
[25] S. Miserere, G. Mottet, V. Taniga, S. Descroix, J.-L. Viovy, L. Malaquin, Lab Chip 12 (10) (2012) 1849–1856.
[26] Y. Ladner, A. Bruchet, G. Crétier, V. Dugas, J. Randon, K. Faure, Lab Chip 12 (12) (2012) 1680–1685.
[27] N.S. Isaacs, K. Neelakantan, Can. J. Chem. 45 (1967) 1597–1600.
[28] A. Bruchet, V. Dugas, I. Laszak, C. Mariet, F. Goutelard, J. Randon, J. Biomed. Nanotechnol. 7 (3) (2011) 415–425.
[29] A. Bruchet, V. Dugas, C. Mariet, F. Goutelard, J. Randon, J. Sep. Sci. 34 (16–17) (2011) 2079–2087.
[30] C. Nguyen Trung, G.M. Begun, D.A. Palmer, Inorg. Chem. 25 (1992) 5280–5287.
[31] K.A. Gshneidner, J.L. Eyring, G.H. Lander, G.C. Chopin, Handbook on the Physics and Chemistry of Rare Earth, in: K.L. Nash (Ed.), Inc. Amsterdam, North Holland, 1994.
[32] D.C. Duffy, H.L. Gillis, J. Lin, N.F. Sheppard, G.J. Kellogg, Anal. Chem. 71 (1999) 4669–4678.
[33] K. Faure, Electrophoresis 31 (2010) 2499–2511.
[34] I. Nischang, J. Chromatogr. A, 1287, 2013, 39–58.
[35] B.S. Lee, Y. Ui Lee, H.-S. Kim, T.-H. Kim, J. Park, J.-G. Lee, J. Kim, H. Kim, W.G. Lee, Y.-K. Cho, Anal. Chim. Acta 428 (2001) 133–142.
[36] D. Connolly, B. Paull, J. Sep. Sci. 32 (15–16) (2009) 2653–2658.